Supporting Information

Hams et al. 10.1073/pnas.1315854111

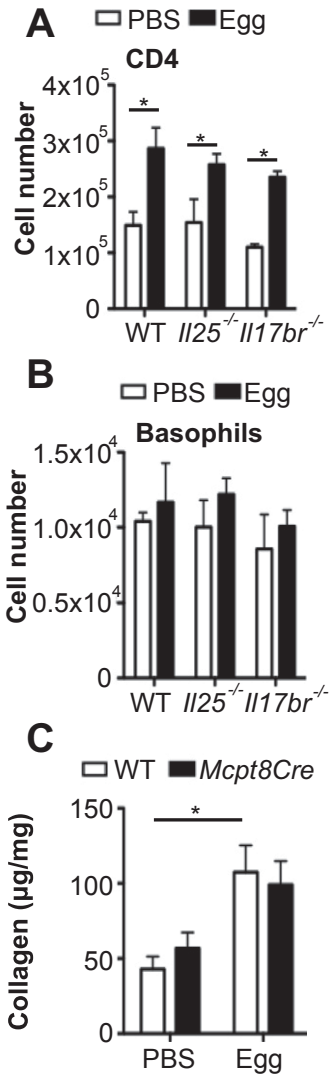

Fig. S1. Cellular infiltration into the lungs in response to *Schistosoma mansoni* egg challenge. Pulmonary granulomas were induced in WT, *Il25*$^{-/-}$ and *Il17br*$^{-/-}$ and *Mcpt8Cre* mice. Absolute numbers of CD4 cells (B220^{-}CD4^{+}) (*A*) and basophils (CD4^{-}CD8^{-}CD19^{-}FcεR1^{+}c-kit^{-}IL-4^{+}) (*B*) were quantified in the lung tissue of unchallenged mice and egg-challenged mice at day 7. (*C*) Total collagen in lung digests expressed per mg of lung protein for WT and basophil-depleted *Mcpt8Cre* mice. Data are representative of mean ± SEM (n = 2–6) from two individual experimental replicates (*P < 0.05).

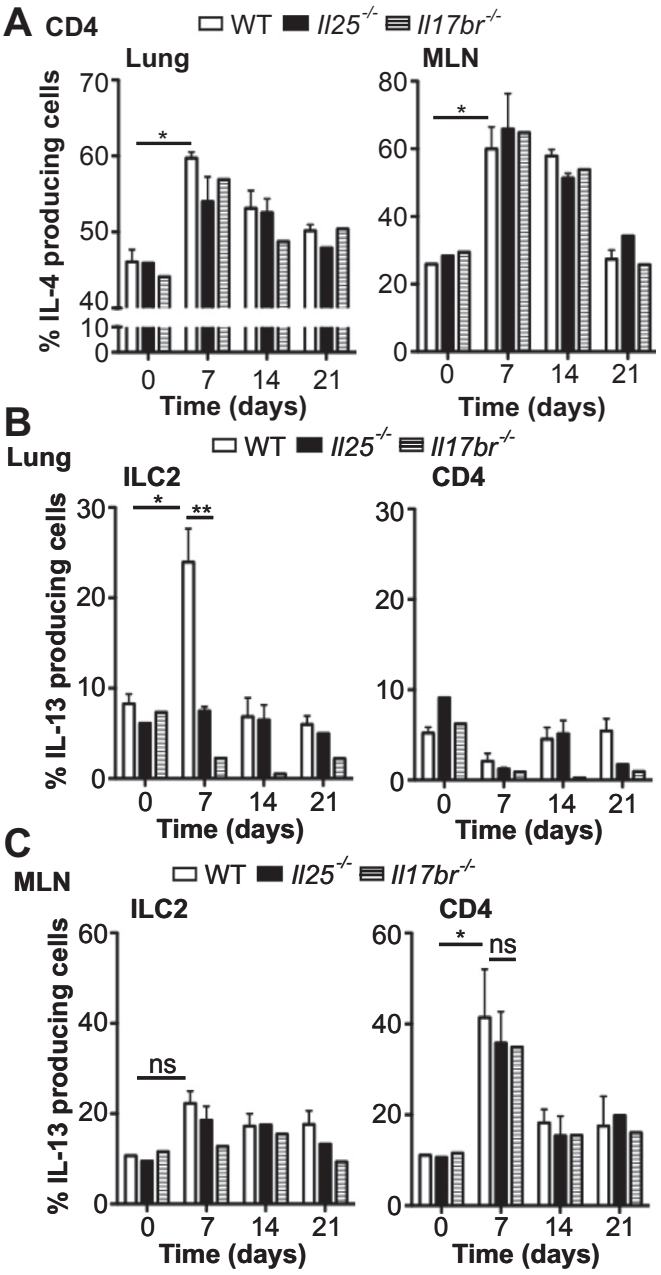

Fig. S2. Cytokine expression in the lungs and mediastinal lymph nodes (MLN) in response to *S. mansoni* egg challenge. Pulmonary granulomas were induced in WT *Il25*-, and *Il17br*-deficient mice. (*A*) The proportion of IL-4$^+$CD4$^+$ T cells in the lung and MLN was quantified at days 0, 7, 14, and 21. The percentage of IL-13$^+$ILC2 (CD3$^-$CD4$^-$CD8$^-$CD19$^-$CD11b$^-$CD11c$^-$Gr-1$^-$FcεR1$^-$F4/80$^-$IL-7Rα$^+$Sca-1$^+$) and IL-13$^+$CD4$^+$ T cells in the lung (*B*) and MLN (*C*) of WT *Il25*$^{-/-}$ and *Il17br*$^{-/-}$ were quantified at days 0, 7, 14, and 21 postegg challenge. Data are representative of mean ± SEM (n = 2–3) from two individual experimental replicates (ns, not significant; *$P < 0.05$).

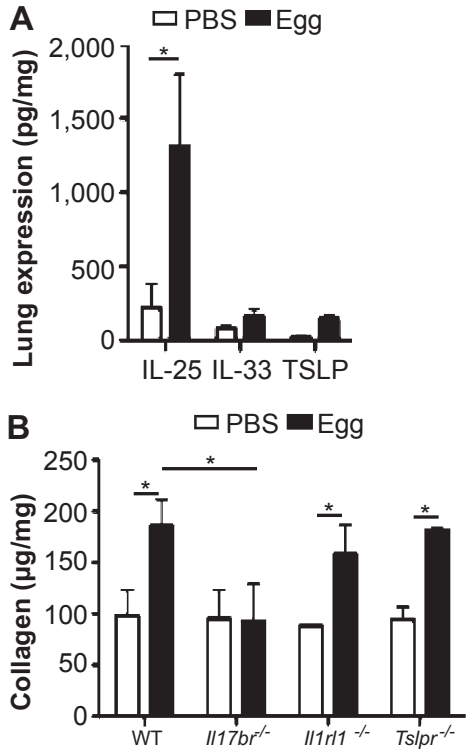

Fig. S3. Expression of IL-25, IL-33, and thymic stromal lymphopoietin (TSLP) in response to egg-induced pulmonary fibrosis. (*A*) Expression of IL-25, IL-33, and TSLP determined in the lungs of WT mice in response to egg-induced fibrosis assessed by ELISA and expressed as picogram (pg) per mg of protein. (*B*) Pulmonary granulomas were induced in WT-, IL-17BR (*Il17br*$^{-/-}$)-, T1/ST2 (*T1/st2*$^{-/-}$)-, and TSLPR (*Tslpr*$^{-/-}$)-deficient mice and total collagen in lung digests expressed per mg of lung protein. Data are representative of mean ± SEM (n = 3–4) from two individual experimental replicates (*P < 0.05, **P < 0.01).

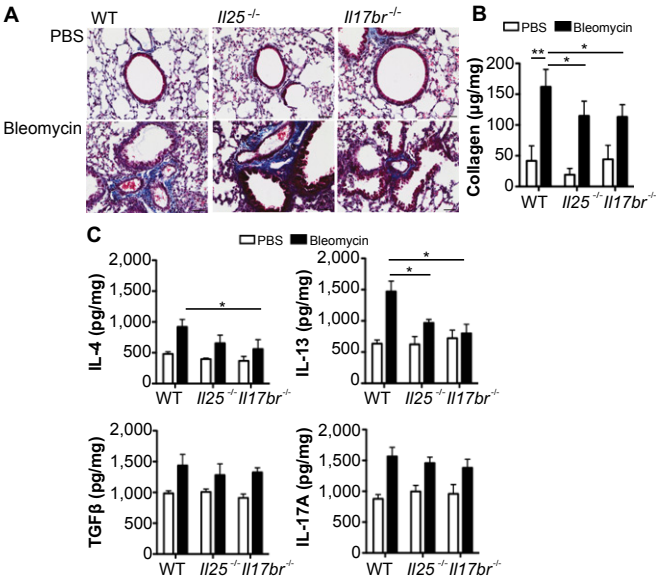

Fig. S4. IL-25–deficient mice have decreased pulmonary collagen deposition in bleomycin-induced pulmonary fibrosis Pulmonary fibrosis was induced in groups of WT, *Il25*$^{-/-}$ and *Il17br*$^{-/-}$ by intratracheal injection of 0.15 U bleomycin. (*A*) Collagen was assayed in the lungs by histology, using Masson's Trichrome (scale, 50 μM) and by (*B*) quantitative analysis. (*C*) Levels of IL-4, IL-13, TGFβ, and IL-17A in the lung were expressed per mg of lung protein. Data are representative of mean ± SEM (n = 6–8) from three individual experimental replicates (*P < 0.05, **P < 0.01).

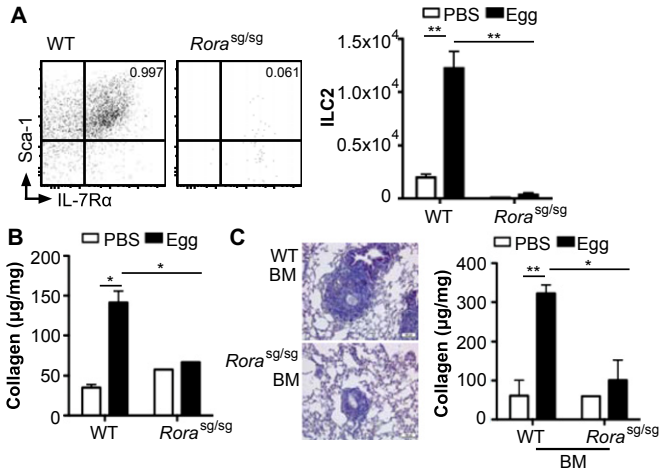

Fig. S5. Mice deficient in the transcription factor RORα show impairment in the generation of ILC2 and pulmonary collagen deposition. (*A*) Frequency of ILC2 ($CD3^-CD4^-CD8^-CD19^-CD11b^-CD11c^-Gr\text{-}1^-Fc\varepsilon R1^-F4/80^-IL\text{-}7R\alpha^+Sca\text{-}1^+$) in the lung of unchallenged WT and *Rora*$^{sg/sg}$ mice. ILC2 expansion in the lungs (*B*) and pulmonary collagen deposition (*C*) in WT and *Rora*$^{sg/sg}$ mice after egg challenge. Bone marrow chimeras were generated using donor cells from WT and *Rora*$^{sg/sg}$ mice and after egg challenge the pulmonary collagen analyzed by histology (scale, 50 μM) and by quantitative analysis (*C*). Data are representative of mean ± SEM (n = 2–4) from three individual experimental replicates (*P < 0.05, **P < 0.01).

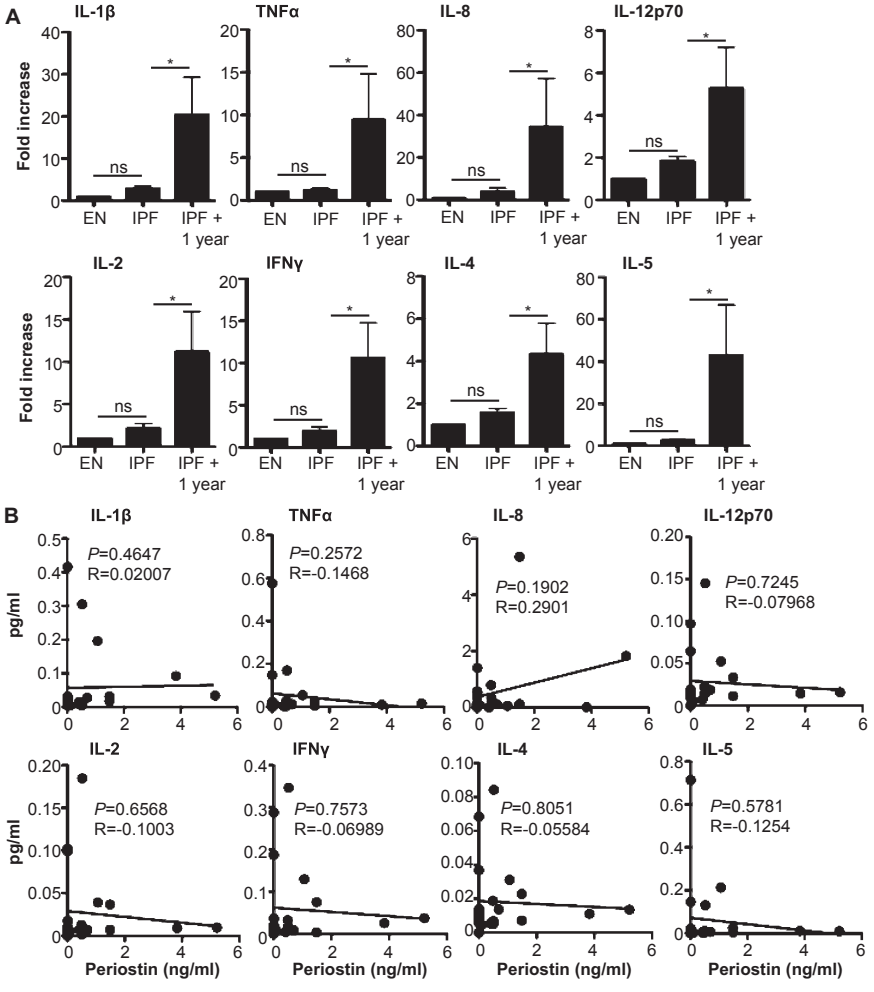

Fig. S6. Cytokine expression in the bronchalveolar lavage (BAL). BAL fluid and lung tissue of idiopathic pulmonary fibrosis (IPF) patients. BAL fluid was collected from patients with IPF at diagnosis and at a 1-y follow-up (IPF + 1 y) and patients diagnosed with erythema nodosum (EN; nonprogressive patients). (*A*) Cytokines in BAL fluid were quantified by ELISA and expressed as fold-increase relative to EN patients. (*B*) Correlation between BAL fluid levels of cytokines and periostin was plotted and Pearson's correlation calculated and displayed on the graph. Data are representative of mean ± SEM (n = 3, EN; n = 14, IPF and IPF + 1 y) (*P < 0.05, **P < 0.01).

Table S1. Characteristics and pulmonary function of IPF subjects at baseline and 12-mo follow-up

Demographic	IPF subjects
No.	14
Sex, M/F, %	64/36
Median age, year range	66 (50–75)
Smoker, ever/never, %	73/27
Physiological, baseline	
FEV1, % predicted	98.7 (74.2–113)
FVC1, % predicted	92.1 (70.7–115)
FEV1/FVC1 ratio	81.8 (73.9–86.9)
T_{CO}, % predicted	51.4 (30.9–67.9)
Disease progression, 12 mo	
FEV1 slope	−0.07 (-19.4–5.9)
FVC1 slope	3.10 (-19.4–8.0)
T_{CO} slope	−4.10 (-22.4–10.6)

Values are presented as median (range). Slope values represent the % change at 12 mo from baseline values. FEV1, forced expiratory volume in 1 s; FVC1, forced vital capacity; T_{CO}, transfer factor–absorption of CO in one breath.